

Bubble Motion under Gravity through Lattice Boltzmann Method

D.M. Nie

Institute of Fluid Mechanics
China Jiliang University
Hangzhou, 310018, China

L.M. Qiu

Institute of Refrigeration and Cryogenics
Zhejiang University
Hangzhou, 310027, China

X.B. Zhang

Institute of Refrigeration and Cryogenics
Zhejiang University
Hangzhou, 310027, China

Abstract—The motion of two bubbles under gravity is numerically studied through the lattice Boltzmann method for the Eotvos number ranging from 1 to 12. The effects of Eotvos number on the bubble coalescence and rising velocity are investigated. It has been found that the uppermost bubble deforms the most because of the maximum drag. In addition, the averaged rising velocity of the bubbles is also studied in this work.

Keywords-lattice Boltzmann method; bubble; coalescence

I. INTRODUCTION

Bubble motion is one of the most common gas-liquid flow phenomena and plays an important role in many industrial applications, such as cavitation fluid machinery, nucleate boiling in reactors and condenser/evaporator [1]. The motion of bubble under gravity is complex due to bubble deformation, coalescence and breakup. Understanding the dynamic interaction between bubbles is an important aspect of the design and operation of many industrial applications.

A number of investigations of the bubble motion in liquid have been conducted in the past [2-5] due to its scientific and engineering importance. In recent decades, the lattice Boltzmann method (LBM) has proved to be a powerful numerical scheme for the simulation of multiphase flow which is based on mesoscopic particle dynamics. Its kinetic nature can provide many of the advantages of molecular dynamics [6]. Several kinds of lattice Boltzmann model for simulating multiphase fluid have been established and applied to the simulations of gas bubbles under gravity successfully. These models include potential method proposed by Shan et al. [7], color method proposed by Rothman et al. [8], and free energy method proposed by Swift et al. [9] and improved by Zheng et al. [10]. The free energy method [10] was proved to be a good tool for the study of two-phase flows with high viscosity ratios and high density ratio. As shown by Gupta et al. [11] and Yu et al. [12], in comparison with the case of single bubble, the motion of multiple bubbles under gravity could be much more complex due to hydrodynamic interactions between bubbles. Besides, the bubble coalescence and

break-up could take place occasionally which have great effect on the motion of multiple bubbles. However, a detailed numerical study of the influence of bubble collision and coalescence on the rising velocity has not been undertaken. It is important to focus on the fundamental understanding of the bubble collision and coalescence when multiple bubbles are rising under gravity. To fulfil this task the LBM proposed by Zheng et al. [10] is adopted in this work to study the rise behavior of multiple bubbles which are initially placed in in-line arrangement. This study will evaluate the coalescence pattern and rising velocity of the bubbles which not only depend on the computational parameters but also depend on the initial arrangements. In addition, the terminal velocity is compared with the result of single bubble under the same conditions to illustrate the influence of multiple bubbles motion.

II. NUMERICAL METHOD

The discrete lattice Boltzmann equations under external forces for the continuity and momentum equations are given by,

$$f_i(x + e_i \Delta t, t + \Delta t) - f_i(x, t) = -\frac{1}{\tau_n} [f_i(x, t) - f_i^{(eq)}(x, t)] + \frac{w_i}{c_s^2} (F + \mu_p \nabla \phi) \cdot e_i \quad (1)$$

where $f_i(x, t)$ is the density distribution function at the i th microscopic velocity e_i , $f_i^{(eq)}(x, t)$ is the equilibrium distribution function, F is the external force (which is gravity in this work), Δt is the time step, τ_n is the relaxation time, c_s is the speed of sound and w_i are the weights related to the D2Q9 model. ϕ is the order parameter that is responsible for the gas-liquid interface. μ_p is the chemical potential, which is defined in the following. The macroscopic variables n and u are determined by the distribution function as follows,

$$n = \sum_i f_i, \quad nu = \sum_i f_i e_i \quad (2)$$

The variables n and u are defined as

$$n = \frac{\rho_L + \rho_G}{2}, \quad \phi = \frac{\rho_L - \rho_G}{2} \quad (3)$$

where L and G are the densities of liquid and gas phase, respectively. The equilibrium distribution functions $f_i^{(eq)}$ are defined as

$$f_i^{(eq)} = w_i A_i + w_i n \left[3\mathbf{u} \cdot \mathbf{e}_i - \frac{3}{2}u^2 + \frac{9}{4}(\mathbf{u} \cdot \mathbf{e}_i)^2 \right] \quad (4)$$

According to Zheng et al. [12], the coefficients are defined as

$$A_0 = \frac{9}{4}n - \frac{15}{4}\left(\phi\mu_\phi + \frac{1}{3}n\right), \quad A_{1-8} = 3\left(\phi\mu_\phi + \frac{1}{3}n\right) \quad (5)$$

The discrete lattice Boltzmann equations for the interface capture equation are given by [12],

$$g_i(\mathbf{x} + \mathbf{e}_i \Delta t, t + \Delta t) = q g_i(\mathbf{x}, t) + (1-q) g_i(\mathbf{x} + \mathbf{e}_i \Delta t, t) - \frac{1}{\tau_\phi} [g_i(\mathbf{x}, t) - g_i^{(eq)}(\mathbf{x}, t)] \quad (6)$$

where q is a constant coefficient, which is determined by,

$$q = \frac{1}{\tau_\phi + 0.5} \quad (7)$$

The macroscopic variable, i.e. the order parameter ϕ , is given by,

$$\phi = \sum_i g_i \quad (8)$$

According to Zheng et al. [12], the chemical potential is computed using,

$$\mu_\phi = A(4\phi^3 - 4\phi^{*2}\phi) - \kappa \nabla^2 \phi \quad (9)$$

where $\phi^* = 0.5(L + G)$, and L and G are the densities of the liquid phase and the gas phase, respectively. A and κ are parameters related to the thickness of the interface layer W and the surface tension coefficient σ , which are expressed as,

$$W = \frac{\sqrt{2\kappa/A}}{\phi^*}, \quad \sigma = \frac{4\sqrt{2\kappa A}}{3} \phi^{*3} \quad (10)$$

The equilibrium distribution functions $g_i^{(eq)}$ are [12],

$$g_i^{(eq)} = A_i + B_i \phi + C_i \phi \mathbf{e}_i \cdot \mathbf{u} \quad (11)$$

where the coefficients A_i , B_i and C_i are defined according to the D2Q5 lattice.

By Chapman–Enskog analysis, the Navier–Stokes equations and an interface evolution equation can be obtained by Eq. (1) and Eq. (6),

$$\frac{\partial n}{\partial t} + \nabla \cdot (n\mathbf{u}) = 0 \quad (12)$$

$$\frac{\partial (n\mathbf{u})}{\partial t} + \nabla \cdot (n\mathbf{u}\mathbf{u}) = -\nabla P + \mu \nabla^2 \mathbf{u} + \mathbf{F} \quad (13)$$

$$\frac{\partial \phi}{\partial t} + \nabla \cdot (\phi \mathbf{u}) = \theta_M \nabla^2 \mu_\phi \quad (14)$$

where M is the mobility, given by $M = q(\tau_\phi - 0.5) \times \tau_\phi$. The viscosity is $\mu = (\tau_\phi - 0.5)n/3$.

III. RESULTS AND DISCUSSION

Three cases are carried out to validate the present computational code. The first is the Laplace law, which is given (for the two-dimensional case) by

$$\Delta p = \frac{\sigma}{R} \quad (15)$$

where p is the pressure jump across the interface, and R is the bubble radius. In this work, the Laplace law is validated by calculating the pressure jump while varying the bubble radius from $R=10$ to $R=80$. Other parameters are fixed at $L=1000$, $G=1$, $\tau_\phi=2$ and $\tau_\phi=400$. The interface layer thickness is set to be $W=4$ for $R < 20$ and $W=5$ for $R \geq 20$. The relaxation times are $\tau_\phi=0.875$ and $\tau_\phi=0.7$. The results are shown in Figure I, which shows good agreement between the numerical results and the analytical solution of Eq.(15).

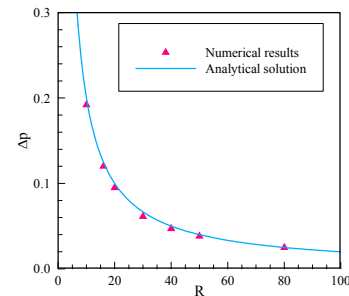


FIGURE I . THE VERIFICATION OF THE LAPLACE LAW.

In this section multiple bubbles motion for both horizontal arrangement and vertical arrangement are investigated in detail. The parameters are fixed at $L=2.6$, $G=1$, $\tau_\phi=0.01$, $W=4.5$, $R=20$ and $\tau_\phi=0.5$. The computational domain is 250×1500 and stationary walls are applied for all boundaries.

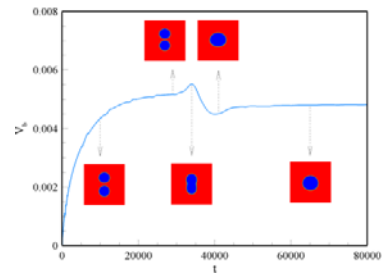


FIGURE II . TIME EVOLUTION OF THE RISING VELOCITY OF TWO BUBBLES FOR $EO=1$.

Figure II shows the time evolution of the rising velocity of two bubbles for $EO=1$. The two bubbles are initially placed in a vertical orientation separated by center to center distance of $2.5R$ initially. As shown in the figure, after an initial period of evolution the velocity becomes constant which indicates that the merged bubble is rising at a constant velocity due to the balance between buoyancy and drag forces. For better understanding the contours of order parameter which visualize the process of bubble collision and coalescence are also

shown in Figure II. It's observed that an oscillation occurs in the bubble velocity before the steady state. Obviously, this oscillation corresponds to the bubble coalescence process. Furthermore, as shown in fig. 3 the terminal velocity is smaller than the velocity before the two bubbles collide and coalesce.

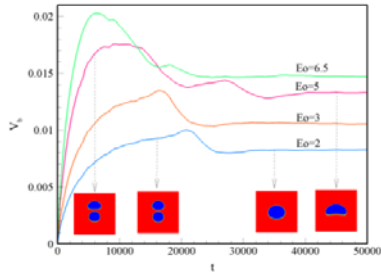


FIGURE III. TIME EVOLUTION OF THE RISING VELOCITY OF TWO BUBBLES FOR DIFFERENT Eo.

The effects of the Eotvos number on the evolution of bubble velocity are shown in Figure III. It's observed that as the Eotvos number increases the bubble velocity increases and the magnitude of oscillation also increases. Moreover, it has been found that in all cases ($1 \leq Eo \leq 12$) the two bubbles would collide and coalesce. The lower bubble always rises at a higher speed than the upper one because it is located at the wake behind the upper bubble. This leads to a smaller drag force for the lower bubble. Since the relative velocity of the bubbles is non-zero, the distance between the two bubbles keeps decreasing with time. Eventually the bubbles come to contact and merge, and soon after form a larger bubble with twice the volume as the initial bubble.

In order to present more insight into the rising process of multiple bubbles under gravity, the terminal velocities of two bubbles for different Eotvos numbers are shown in Figure IV. For the purpose of comparison, the results of a single bubble under the same conditions are also shown in the figure. It's unexpected that for very low Eotvos numbers such as $Eo \leq 3$, the terminal velocities of two bubbles are a little larger than those of a single bubble, as can be seen in Figure 4. The reason is not clear. However, for high Eotvos numbers such as $Eo > 6$ the terminal velocities are similar for all cases, indicating that the influence of the wall boundaries on the terminal velocity is insignificant. Moreover, the bubble coalescence strongly affects the time evolution of bubble velocity, but has little influence on the terminal velocity.

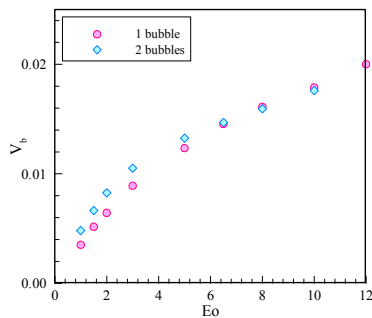


FIGURE IV. THE TERMINAL RISING VELOCITY FOR DIFFERENT EOTVOS NUMBERS.

IV. CONCLUSION

In this work the lattice Boltzmann method is used to simulate the motion of two bubbles under gravity. The Laplace law has been adopted to validate the present method. The vertical arrangement is taken into account in the simulations with Eotvos number ranging from 1 to 12. The uppermost bubble deforms the most because of the maximum drag. In addition, after the coalescence a larger bubble is formed eventually. The terminal velocity of two bubbles is a little larger than that of one bubble under the same conditions. However, the terminal velocity is similar for all cases when the Eotvos number is large.

ACKNOWLEDGEMENTS

This work was supported by the National Program on Key Basic Research Project of China (grant no. 2011CB706501) and the National Natural Science Foundation of China (grant no. 11272302).

REFERENCES

- [1] Dijkink, R. J., van der Dennen, J. P., Ohl, C. D., Prosperetti, A., The 'acoustic scallop': a bubble-powered actuator. *Journal of Micromechanics and Microengineering*, 16, pp. 1653–1659, 2006.
- [2] Van Wijngaarden, L., Vossers, G., Mechanics and physics of gas bubbles in liquids: a report on Euromech 98. *Journal of Fluid Mechanics*, 87, pp. 695–704, 1978.
- [3] Batchelor, G.K., The stability of a large gas bubble rising through liquid. *Journal of Fluid Mechanics*, 184, pp. 399–422, 1987.
- [4] Krishna, R., van Baten, J. M., Simulating the motion of gas bubbles in a liquid. *Nature*, 398, pp. 208, 1999.
- [5] Joseph, D.D., Rise velocity of a spherical cap bubble. *Journal of Fluid Mechanics*, 488, pp. 213–223, 2003.
- [6] Takada, N., Misawa, M., Tomiyama, A., Hosokawa, S., Simulation of bubble motion under gravity by Lattice Boltzmann Method. *Journal of Nuclear Science and Technology*, 38(5), pp. 330–341, 2001.
- [7] Shan, X., Chen, H., Lattice Boltzmann model for simulating flows with multiple phases and components. *Physical Review E*, 47, pp. 1815–1819, 1993.
- [8] Rothman, D.H., Keller, J.M., Immiscible cellular-automaton fluids. *Journal of Statistical Physics*, 52, pp. 1119–1127, 1988.
- [9] Swift, M.R., Osborn, W.R., Yeomans, J.M., Lattice Boltzmann simulation of non-ideal fluids. *Physical Review Letter*, 75, pp. 830–833, 1995.
- [10] Zheng, H.W., Shu, C., Chew, Y.T., A lattice Boltzmann model for multiphase flows with large density ratio. *Journal of Computational Physics*, 218, pp. 353–371, 2006.
- [11] Gupta, A., Kumar, R., Lattice Boltzmann simulation to study multiple bubble dynamics. *International Journal of Heat and Mass Transfer*, 51, pp. 5192–5203, 2008.
- [12] Yu, Z., Yang, H., Fan, L.S., Numerical simulation of bubble interactions using an adaptive lattice Boltzmann method. *Chemical Engineering Science*, 66(14), pp. 3441–3451, 2011.